

Thermal, Morphological, and Mechanical Properties of Regular and Waxy Maize Starch Films Reinforced with Cellulose Nanofibers (CNF)

Vanessa Soltes de Almeida^a, Bárbara Ruivo Válio Barretti^a, Vivian Cristina Ito^b, Lucca Malucelli^c,

Marco Aurélio da Silva Carvalho Filho^c, Ivo Mottin Demiate^a, Luís Antonio Pinheiro^d,

Luiz Gustavo Lacerda^{a*} 

^aUniversidade Estadual de Ponta Grossa (UEPG), Programa de Pós-Graduação em Ciência e Tecnologia de Alimentos, Ponta Grossa, PR, Brasil

^bUniversidade de São Paulo (USP), Escola Superior de Agricultura Luiz de Queiroz, Departamento de Agroindústria, Alimentos e Nutrição, Piracicaba, SP, Brasil

^cUniversidade Positivo (UP), Programa de Pós-Graduação em Biotecnologia Industrial, Curitiba, PR, Brasil

^dUniversidade Estadual de Ponta Grossa (UEPG), Engenharia de Materiais, Ponta Grossa, PR, Brasil

Received: October 18, 2019; Revised: January 31, 2020; Accepted: March 26, 2020

Biodegradable films were prepared using regular and waxy starch and reinforced with cellulose nanofibers (CNF) from eucalyptus. Both films were characterized by their optical, structural, barrier, thermal and mechanical properties. The films presented a homogeneous, smooth surface without bubbles or cracks and good handling characteristics. Both films showed a mixture of B and V-type diffraction patterns. The water solubility of the samples decreased after the incorporation of nanocellulose. The water vapor permeability for both sources significantly reduced after incorporating nanocellulose at 0.5% and 1%. It is possible to observe that the addition of CNF increased the thermal stability of the starch films. On the other hand, the incorporation of nanocellulose improved either the mechanical resistance of the starch films.

Keywords: Amylose, biodegradable films, mechanical resistance, nanocellulose, thermoplastic.

1. Introduction

Global ecological and environmental challenges, such as the increase in non-biodegradable waste material and the difficulty in recycling most of the synthetic packaging have been demanding the need for renewable sources to be increasingly used^{1,2}. Starch films are a class of promising biodegradable polymers in the market, as alternatives to the use of petrochemical derivatives³.

Starch is the most widely employed in the elaboration of films, due to its low cost and abundance in nature⁴. Features great capability to form a colorless and transparent polymer matrix, and it is also a heterogeneous material containing different concentrations of amylose and amylopectin⁵. The amylose content in waxy starch is lower than 5%, whereas ranging from regular starch 15-30% and high amylose starch 35-70%⁶.

According to Wang et al. (2015)⁷ amylose content is important for the structural stability of starch and the formation of biodegradable films, with linear chains and a network stabilized by hydrogen bonds. Its content influences of their tensile strength and elongation^{8,9}. In contrast, the polymeric chains of amylopectin can be highly tangled together due to their branching and shorter length, leading to the formation of inter-chain hydrogen bonds⁵.

However, the application of starch film is limited by its mechanical properties and barrier ability. These films are highly hygroscopic, loosely flexible and brittle¹⁰. Moreover, retrogradation of the mobile starch chains leads to an undesired

change in thermomechanical properties¹¹. To enhance the properties of these films, the additives, such as cellulose nanofibers (CNF) can be used to improve the mechanical, barrier, physical and thermal properties of starch due to the nanometric size and high crystallinity of cellulose^{12,13}.

Natural fibers are produced in billions of tons annually worldwide and are therefore abundant, inexpensive and readily available. The nano cellulosic structure embedded in the polymeric matrices makes the films more mechanically resistant while still keeping the process environmentally-friendly and sustainable¹⁴. Therefore, the objective of this work was to investigate the thermal, morphological, and mechanical properties of regular and waxy maize starch films reinforced with cellulose nanofibers (CNF). The films were produced by casting using glycerol (as plasticizer) and CNF (as an additive), in which the last was added after starch gelatinization.

2. Experimental

2.1 Materials

The regular maize starch containing 27% amylose content, 33.4% relative crystallinity and 7.4 J/g gelatinization enthalpy and waxy maize starch containing 0.8% amylose content; 37.7% relative crystallinity and 11.4 J/g gelatinization enthalpy, used in the experiments were kindly donated by Ingredion Brazil Industrial Ingredients LTDA, located in Balsa Nova, Paraná, Brazil. Glycerol (PA) was used as a plasticizer. The remaining reagents were of analytical grade.

*e-mail: lglacerda@uepg.br

2.2 Cellulose nanofiber (CNF) preparation

Bleached Eucalyptus Pulp (BEP) used in the experiments were kindly donated by Positivo University- Paraná- Brazil as a raw material for CNF preparation as follows. BEP was dispersed in 2L of distilled water at 1% using a lab mixer and ground in an MKCA 6-2 ‘Supermasscolloider’, Masuko Sangyo (Kawaguchi, Japan) for 25 passes. After CNF production, CNF was oven-dried until constant weight¹⁵. Zeta potential of the eucalyptus nanocellulose suspension showed a value of -23.1 mV and an average particle size of 14.24 nm in previous analysis.

2.3 Preparation of starch and nanocellulose films

The films were prepared according to the procedure described in Fan et al. (2016)¹⁶ with the following modifications. In brief, the films were composed of starch (7.0 g in dry basis), glycerol as the plasticizer (3.0 g) and 100 mL of deionized water. The dispersion was stirred manually in a beaker-type flask and heated for 7 min on a heating plate. After starch gelatinization (approximately at 90°C) the system was cooled down to 40°C and the CNF suspensions were added at 0, 0.5, 1 and 1.5%. Before the characterization tests, the films were conditioned at 25°C for 5 days in a desiccator with a relative humidity of 53% (using a saturated solution of MgNO₃).

2.4 Moisture content of the films

The moisture content of samples of the films (approximately 2x2 cm) was determined, in triplicate, by gravimetric analysis measuring the weight loss of the films before and after drying in a laboratory oven at 105°C for 24 h.

2.5 Solubility in water

The films’ solubility (S) was calculated using the method described by Pelissari et al. (2017)¹⁷ with modifications. Initially, three discs of 4cm² were dried in a laboratory oven. The samples were weighed, to obtain the initial dry weight (W_i), and were then immersed into 50mL water at 25°C for 24h, kept under continuous mechanical stirring using an orbital shaker (Novatecnica-NT 714, Piracicaba, Brazil). Then, the water containing the discs was filtered, the insoluble matter dried at 105°C for 24 h, and the resulting material weighed to obtain its final dry weight (W_f). The analyses were carried out in triplicate, and the solubility in water (%) of the films was calculated according to Equation 1:

$$S = \frac{W_i - W_f}{W_i} \quad (1)$$

in which W_i is the initial dry weight (g), and W_f is the final dry weight of the sample (g).

2.6 Water vapor permeability (WVP)

Each film sample was sealed over a circular opening (area = 0,000707m₂) in a permeation cell that was conditioned at 25°C in a desiccator. As outlined in the standard method, anhydrous calcium chloride (0% Relative Humidity) was placed inside the cell, while saturated sodium chloride solution (75% Relative Humidity) was placed in the desiccator. Owing to the vapor pressure gradient across the film, the

water vapor diffused continuously through the film can be determined from the weight gained by the permeation cell. The fluctuation in cell weight of the cell was measured for 4 days^{16,18,19} and the WVP was calculated using Eq. 2 extracted from a recent study¹⁸:

$$WVP = \frac{\Delta m}{(\Delta t \times A \times X \Delta P)} (d) \quad (2)$$

in which WVP refers to water vapor permeability, d to film thickness (m), Δm to the weight increase of the cup (g), A to the exposed area (m²), Δt to the time for permeation (s), and ΔP to the difference in water vapor pressure across the film (1753.55 Pa). All measurements were carried out in triplicate.

2.7 Thickness of the films

The thickness of the prepared films was measured using a digital micrometer (Mitutoyo, Japan, 0.001 mm accuracy). The reported thickness values are the mean values of ten film specimens. The average value of each film was used to calculate their tensile properties and the WVP.

2.8 Mechanical properties

Tensile Strength (TS), Elongation at break (E) and Young’s Modulus (YM) of the films were cut in thin rectangular strips (7x0.5cm) and measured ten times on each film using a Shimadzu AG-I 10 KN. Self-tightening roller grips were used to perform the tensile tests. The initial distance between the grips and the initial velocity was adjusted to 50 mm and 25 mm/min, respectively. The mechanical properties of the films were calculated using the average thickness of each sample²⁰.

2.9 Morphological analysis

The morphology of all films was analyzed by field emission gun-scanning electron microscopy (FEG-SEM) in a MIRA 3 (Tescan, Czech Republic). The samples were prepared with gold plating, using 15 kV voltage and approximately 2 kx magnification to obtain the images obtained in the Image J software (Image J 1.47 to WindowsTM)²¹.

2.10 Thermogravimetric analysis (TGA)

The thermal stability of the film samples was determined by thermogravimetric analysis DTG-60 equipment (Shimadzu, Japan) under synthetic airflow of 150 mL/min with a heating rate of 10°C/min from 30 to 600°C. Each sample was weighed around 7.0 ± 2 mg and placed in open α-alumina crucible (BET et al., 2018). The percentages of mass loss and the DTG curves were obtained using TA-60 WS data analysis software.

2.11 X-ray diffraction (XRD)

The X-ray diffractograms (XRD) were obtained using an X-ray diffractometer (Ultima IV, Rigaku, Japan) with CuKα radiation (λ = 1.5418Å), a tension of 40kV and an electric current of 20mA. Film samples were cut into small pieces (2x2 cm) and maintained in a desiccator with silica gel (0%RH) for 5 days. Then, the analyses were performed at 20°C in an angular range of 3-40° (2θ), scanning speed of 2°/min, and a step of 0.02°²².

2.12 Statistical analysis

The results are expressed as the mean \pm standard deviation and were analyzed using Action Stat 3.3 software (Estatcamp, Sao Paulo, Brazil). One-way analysis of variance (ANOVA) was used to study the influence of moisture content, solubility in water, thickness, water vapor permeability and mechanical properties on film properties. Tukey's test was conducted to determine the differences between the means at a 95% confidence level ($p < 0.05$).

3. Results and Discussion

3.1 Characterization of the films

The moisture, solubility, WVP, thickness, and mechanical properties of regular and waxy maize starch films reinforced by nanocellulose from eucalyptus are shown in Table 1. The moisture content was significantly reduced for the regular and waxy starch CNF-reinforced films. Pelissari et al. (2017)¹⁷ also observed a decrease in humidity after the addition of nanoparticles in banana starch films. The same behavior was reported by Li et al. (2015)⁹ in pea starch films. This reduction may be explained by the fact that nanofibers are less hydrophilic compared to starch²³.

The water solubility also decreased after the incorporation of nanocellulose, especially for the regular maize starch films. The lowest values found were for N2 and W2, which contained 1% of nanocellulose compared to their controls (Table 1). Several researchers observed that the addition of nanocomposites can reduce the solubility in aqueous medium of starch-composite films^{17,24,25}.

The WVP for both regular and waxy starch sources was significantly lower for N1 and N2 compared, and W1 and W2, compared to their respective controls (Table 1). This reduction indicates an improvement in the barrier properties of the films and may be related to the nanometric size of the particles added as reinforcement, therefore improving their dispersion in the starch matrix and making more homogeneous

films¹⁶. Also, the addition of nanocomposites probably forms a barrier to water passage, resulting in a more tortuous path for moisture transfer^{9,26}. However, as nanocellulose was added above the 1% threshold for both N3 and W3, resistance to moisture transfer decreased. This may have been due to a possible aggregation of nanocellulose, thus resulting in lower interaction with the starch matrix affecting the integrity and resistance to moisture of those films^{9,27}.

The film thickness ranged from 0.071 to 0.078 μm and no significant difference was observed for the studied samples because the weight of the film suspensions that were poured on polystyrene plates was the same for all cases. Maintaining film thickness uniformity is important for good repeatability during mechanical characterization, as uniform thickness is the basis for determining various film functional variables¹⁶.

The mechanical properties of thermoplastics depend not only on the shape, alignment, quantity, and size of nanoparticles but also on the ability of the polymeric matrix to transfer stress²⁸. Regular maize starch films showed better maximum tensile strength compared to waxy starch films, due to their higher amylose content. The extensive and linear structure chain enables interaction with hydrogen bonds, which makes it capable of producing stronger films compared to the structure of amylopectin, which has a short, highly branched chain that reduces entanglement and makes films more fragile^{8,29}.

The highest values for TS may be attributed to the improved dispersion in the starch matrix³⁰ and the good compatibility and formation of hydrogen bonds between starch and nanocellulose¹⁶. Those factors probably contributed to the stress transfer from the matrix to the nanoparticles, therefore improving the films' resistance^{13,23,25,30,33}.

As it can be seen from Table 1 the results showed a significant increase in the maximum TS from 3.99 to 6.58 MPa after the addition of eucalyptus nanocellulose into regular maize starch films, presented better mechanical properties values than those found by Fan et al. (2016)¹⁶, who also worked with regular maize starch films. There was an increase

Table 1. Moisture content, solubility in water, water vapor permeability (WVP) and mechanical properties of regular and waxy maize starch films reinforced with cellulose nanofibers (CNF).

Regular Maize Starch							
Sample film	Moisture content (%)	Solubility in water (%)	WVP x 10 ⁻⁹ (g/msPa)	Thickness (μm)	Mechanical Properties ^d		
					TS (MPa)	E (%)	YM (MPa)
N0	29.06 ^a \pm 0.01	22.86 ^a \pm 0.02	1.39 ^a \pm 0.02	0.076 ^a \pm 0.01	3.99 ^c \pm 0.36	59.75 ^a \pm 2.66	299.00 ^b \pm 10.39
N1	25.87 ^b \pm 0.01	17.88 ^{bc} \pm 0.01	1.20 ^b \pm 0.04	0.077 ^a \pm 0.01	5.95 ^b \pm 0.38	49.19 ^b \pm 5.88	956.89 ^a \pm 13.68
N2	26.77 ^b \pm 0.01	16.02 ^c \pm 0.01	1.16 ^b \pm 0.04	0.073 ^a \pm 0.01	6.58 ^a \pm 0.57	62.37 ^a \pm 3.64	1085.26 ^a \pm 14.98
N3	27.46 ^{ab} \pm 0.01	20.23 ^{ab} \pm 0.01	1.32 ^a \pm 0.02	0.078 ^a \pm 0.01	5.96 ^b \pm 0.52	45.08 ^b \pm 3.01	906.46 ^a \pm 25.87
Waxy Maize Starch							
Sample film	Moisture content (%)	Solubility in water (%)	WVP x 10 ⁹ (g/msPa)	Thickness (mm)	Mechanical Properties ^d		
					TS (MPa)	E (%)	YM (MPa)
W0	27.54 ^a \pm 1.65	32.85 ^a \pm 0.01	1.42 ^a \pm 0.02	0.073 ^a \pm 0.01	2.06 ^c \pm 0.19	133.39 ^a \pm 11.50	1209.91 ^a \pm 9.06
W1	24.70 ^b \pm 3.32	29.58 ^{ab} \pm 0.01	1.11 ^b \pm 0.04	0.071 ^a \pm 0.01	2.33 ^{ab} \pm 0.35	99.35 ^b \pm 13.61	1122.32 ^a \pm 10.94
W2	25.35 ^{ab} \pm 1.83	27.02 ^b \pm 0.01	1.21 ^b \pm 0.04	0.074 ^a \pm 0.01	2.42 ^a \pm 0.11	93.84 ^b \pm 7.63	1087.25 ^a \pm 13.21
W3	24.85 ^b \pm 0.55	30.47 ^{ab} \pm 0.01	1.39 ^a \pm 0.06	0.072 ^a \pm 0.01	2.15 ^{bc} \pm 0.10	88.85 ^b \pm 2.63	1110.19 ^a \pm 7.16

Note: N0 = regular starch film with 0% nanocellulose; N1 = regular starch film with 0.5% nanocellulose; N2 = regular starch film with 1% nanocellulose; N3 = regular starch film with 1.5% nanocellulose; W0 = waxy starch film with 0% nanocellulose; W1 = waxy starch film with 0.5% nanocellulose; W2 = waxy starch film with 1% nanocellulose; W3 = waxy starch film with 1.5% nanocellulose. ^{a,b,c} Different letters in the same column indicate significant differences ($p \leq 0.05$) between means (Tukey test). ^d TS = tensile strength; E = elongation; YM = Young's modulus.

in TS from 2.06 to 2.42 MPa for waxy maize starch films. According to Li et al., (2014)³⁴ the addition of cellulose strengthens the starch polymer matrix which leads to the increased strength of biodegradable films.

The use of over 1% nanocellulose (1.5%) led to a decrease in tensile strength (Table 1), although it was still higher than the CNF-free films. This reduction is probably due to the aggregation of nanocellulose to a discontinuous and heterogeneous phase, which consequently decreased the films' mechanical properties^{4,16,30}.

The addition of CNF in films may favor increased tensile strength and generally decreased elongation at break (E)^{26,35}. Decreased E was observed for the waxy starch film samples after incorporation of nanocellulose, while for regular starch films it was observed a decrease in only for N1 and N3. Lower elongation values indicate that the obtained films have less flexibility¹⁶.

All CNF-added regular starch films showed an increase in YM. On the other hand, the waxy maize starch films did not show a significant difference between the samples indicating that the incorporation of nanocellulose did not interfere in this parameter. Waxy maize starch films showed higher values of elongation at rupture (E) when compared to regular starch films, in which higher values indicate that the films have higher flexibility¹⁶.

3.2 Morphological analysis

The regular and waxy maize films presented homogeneous, smooth surface, bubble or crack-free and good handling characteristics. The micrographs suggest good compatibility between the nanocellulose and the matrix, as indicated by the homogeneous surface of the films (Figure 1). However, it is possible to observe smooth inhomogeneous clusters in micrographs N3, W1, and W3. According to Manoel et al.

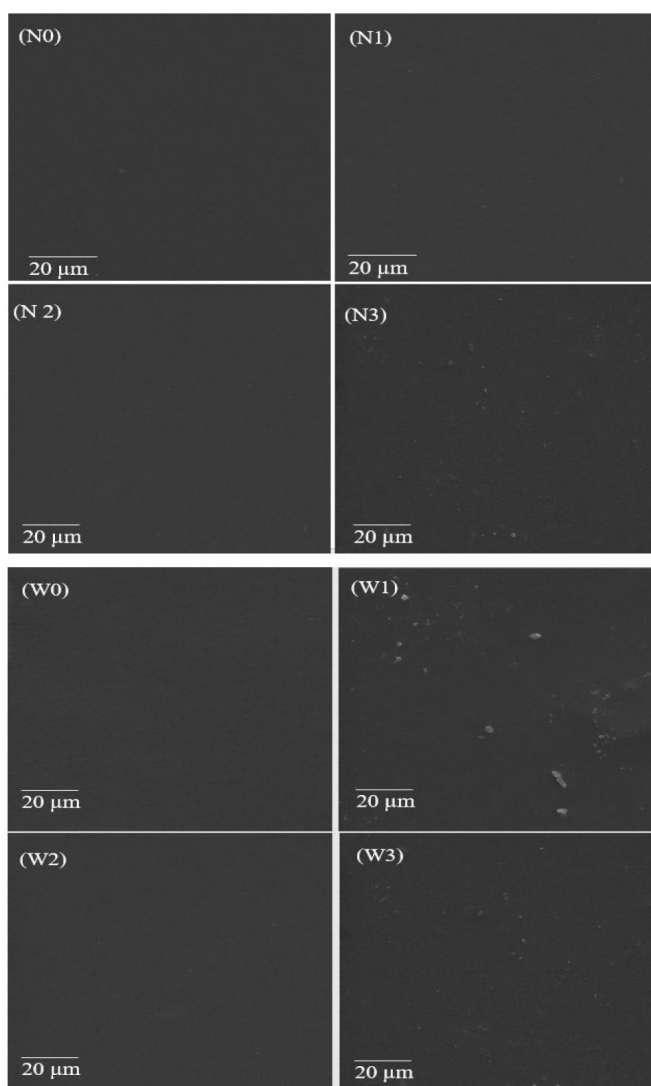


Figure 1. Morphological analysis of the films. Note: N0 = regular starch film with 0% nanocellulose; N1 = regular starch film with 0.5% nanocellulose; N2 = regular starch film with 1% nanocellulose; N3 = regular starch film with 1.5% nanocellulose, W0 = waxy starch film with 0% nanocellulose; W1 = waxy starch film with 0.5% nanocellulose; W2 = waxy starch film with 1% nanocellulose; W3 = waxy starch film with 1.5% nanocellulose.

(2017)⁶, this fact can occur due to a possible formation of bubbles and/or partial gelatinization.

According to Mali, Grossmann, and Yamashita, (2010)³⁶, the higher the amylose content in the starch source, the better is the formation of the biodegradable film. The amylose content within the studied starch sources was 27 and 0.8% for regular and waxy starch, respectively, which are characteristic for these sources³⁷.

It was observed that the starch granules were gelatinized and formed a continuous phase with glycerol. No visible aggregation of nanocellulose and microphase separation were observed in the produced films. Morphological surface similar was found by Basiak; Debeaufor and Lenart (2016)¹⁸, when analyzing wheat starch films.

Melo, Aouada, and Moura (2017)³⁸ reported a decrease in the number of formed pores in nanocomposites incorporated films which increased their compaction and mechanical properties.

Li et al. (2015)⁹ observed that the surface of the control film was smooth and compact, while the films became

rougher as the nanocellulose content increased. Zheng et al. (2009)³⁹ reported that nanocomposites containing 2% pea starch nanocrystals showed a fractured morphology with some fine and dense impressions.

3.3 Thermogravimetric analysis (TGA)

The thermal decomposition under the oxidative atmosphere of the starch films was investigated. Both thermogravimetry (TGA) and first-derivative thermogravimetric (DTG) curves were obtained, as shown in Figure 2 and Figure 3. All TG curves showed similar profiles and four mass loss steps.

The first decomposition was observed and regularly attributed to moisture removal^{40,41}. After this step, it is possible to observe in the temperature range between 180 and 250°C, an evident mass loss due to the decomposition of the glycerol-rich phase that also contains starch. Amylose-rich starches, such as regular maize ones were reported to have a maximum extent of plasticization, due to its minor content in rigid linear chains that helps the glycerol-starch interaction. Starch

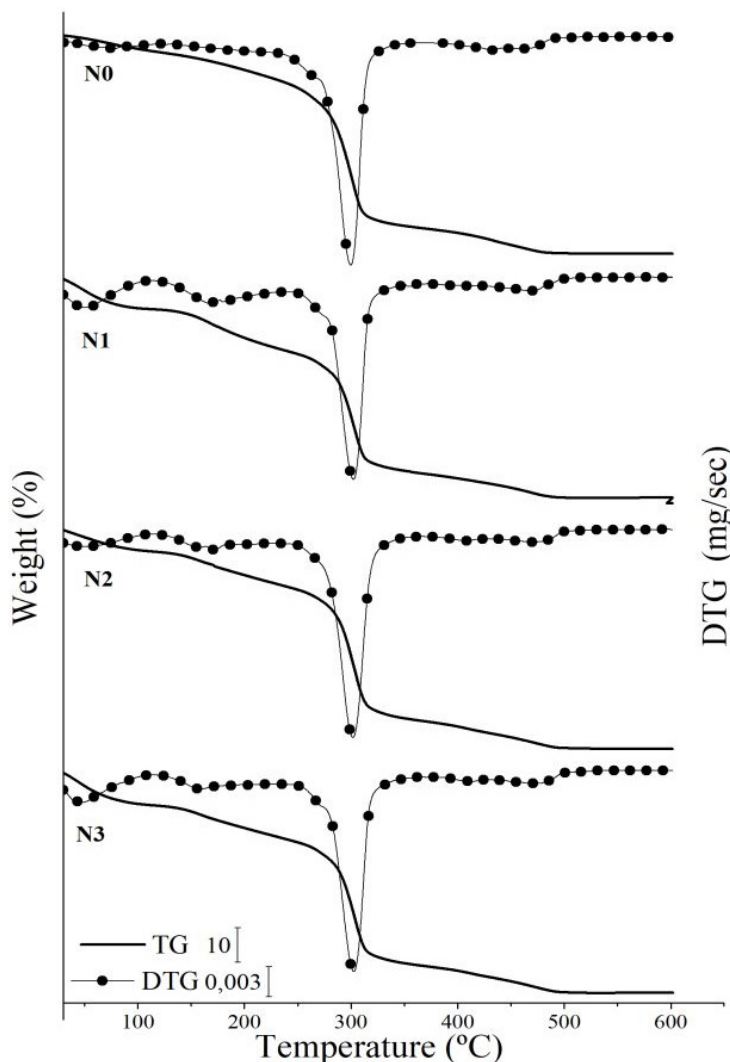


Figure 2. TGA curves and DTG of regular maize starch films. Note: N0 = regular starch film with 0% nanocellulose; N1 = regular starch film with 0.5% nanocellulose; N2 = regular starch film with 1% nanocellulose; N3 = regular starch film with 1.5% nanocellulose.

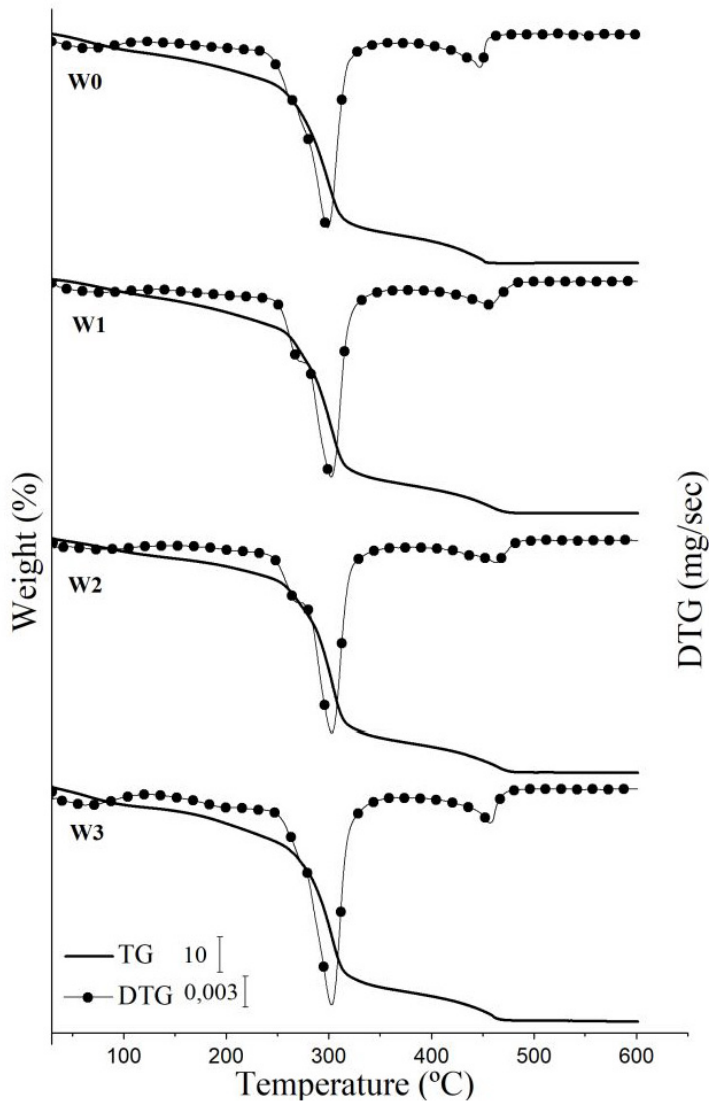


Figure 3. TGA curves and DTG of regular and waxy maize starch films. Note: W0 = waxy starch film with 0% nanocellulose; W1 = waxy starch film with 0.5% nanocellulose; W2 = waxy starch film with 1% nanocellulose; W3 = waxy starch film with 1.5% nanocellulose.

samples submitted to TGA analysis normally presents a step of mass stability from around 180 to 250°C⁴².

The regular maize starch films had a mass loss between 21-31%, which was significantly higher than the one observed for waxy maize films (16-22%) in the same temperature range (30-250°C). The addition of glycerol affects the intra and intermolecular links of the starch because of the strong hydrogen bonds formed between the hydroxyl groups of starch chains and glycerol. Therefore, it is easier to degrade the polymer chains in the presence of glycerol or other plasticizer agents⁴³. On the other hand, this behavior differs in waxy starches considering it is virtually amylose-free. It is possible to observe that the addition of CNF increased the thermal stability of the CNF-composite films provided that only up to 1% CNF is added.

The third mass loss, between 250 and 350°C, refers to the starch-glycerol matrix thermal degradation. Mass loss suggests the greater the number of molecules of glycerol

linked in the plasticized starch phase, the higher is the mass loss in this same temperature range⁴⁴. All samples showed a mass loss around 64% in this temperature range. Finally, the fourth stage (around 350°C) corresponds to the oxidation of the partially decomposed starch and is represented by a mass loss around 10-15% yielding less than 1% ash.

3.4 X-ray diffraction (XRD)

The CNF-added regular and waxy maize starch films displayed a mixture of B and V-type crystal types (Figure 4).

Also, it was possible to observe an entirely amorphous structure in the thermoplastic waxy starch film. This result is consistent with Wang et al. (2017)⁴⁵, reporting that the crystallinity content of starch films increased with high amylose content, while films based solely on amylopectin were amorphous.

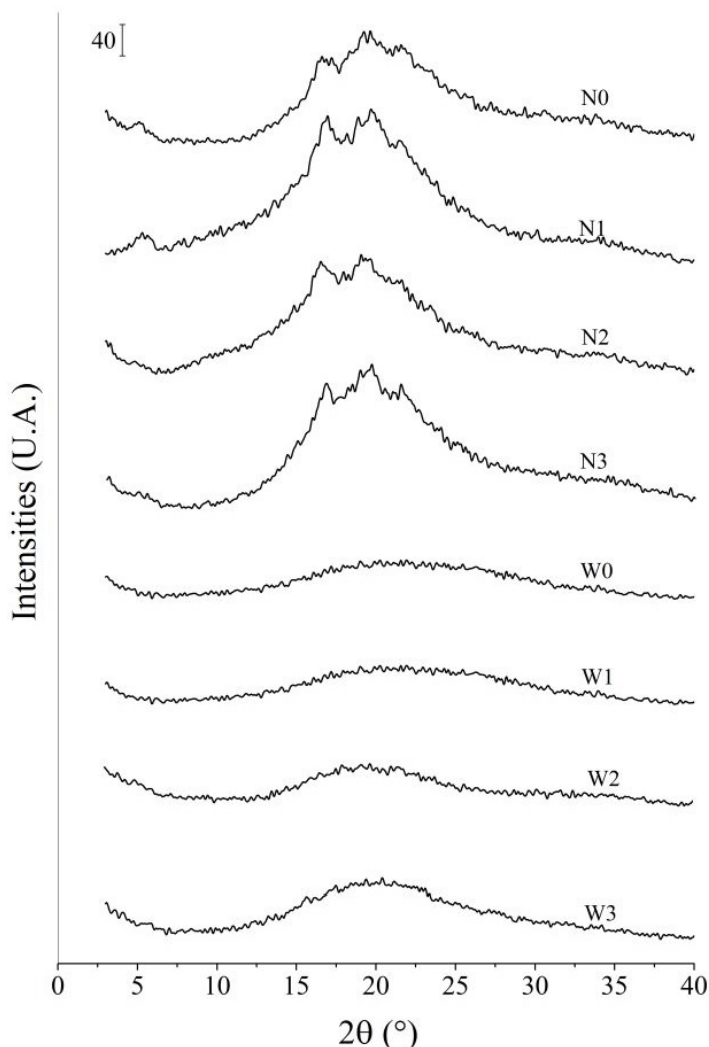


Figure 4. X-ray diffractograms of starch samples and films. Note: N0 = regular starch film with 0% nanocellulose; N1 = regular starch film with 0.5% nanocellulose; N2 = regular starch film with 1% nanocellulose; N3 = regular starch film with 1.5% nanocellulose, W0 = waxy starch film with 0% nanocellulose; W1 = waxy starch film with 0.5% nanocellulose; W2 = waxy starch film with 1% nanocellulose; W3 = waxy starch film with 1.5% nanocellulose.

According to Šárka and Dvořáček (2017)⁴⁶, amylose-rich films are more prone to recrystallization, this justifies the presence of peaks in films based on regular maize starch (N0, N1, N2, and N3). Besides, the formation of crystalline structures in thermoplastic starch depends on the starch source, the amylose/amylopectin ratio, and the degree of branching and the length of the amylopectin outer chains².

4. Conclusion

The moisture content, water solubility, and water vapor permeability have been significantly reduced by the presence of CNF for both regular starch films and waxy starch films. It was possible to observe that the addition of CNF increased the thermal stability of the films since only 1% of the suspension is added. A significant effect was also observed on the mechanical properties. Compared with the control film, the regular starch and waxy starch films showed that the nanocomposites RM increased with the addition of

cellulose nanofibers and the AR had a decrease in their values. Eucalyptus CNF was found to be efficient in improving the barrier, the mechanical and thermal properties of regular and waxy starch films. The use of this nanofiber represents an interesting route to produce more resistant starch-based materials because the inclusion of nanocellulose resulted in an important enhancement of their mechanical properties, therefore suggesting their potential for use as packaging materials and in biodegradable films.

5. Acknowledgments

The authors are deeply grateful to the Fundação Araucária, Coordination for the Improvement of Personnel in Higher Level (CAPES), CNPq (155859/2018-8) for funding and C-LABMU-UEPG for the infrastructure. IMD, LAP e LGL are research fellows from CNPq and are grateful for financial support.

6. References

- Gomes ÁVR, Gonçalves FCP, Silva MQ Jr, Leite RHL, Santos FKG, Aroucha EMM. Effect of Carnauba Wax and Coconut Fiber Contents on tensile properties of corn starch-based biocomposites. *Mater Res*. 2019;22:1-7.
- Pelissari FM, Andrade-Mahecha MM, Sobral PJA, Menegalli FC. Comparative study on the properties of flour and starch films of plantain bananas (*Musa paradisiaca*). *Food Hydrocoll*. 2013;30:681-90.
- Rhim J-W, Park H-M, Ha C-S. Bio-nanocomposites for food packaging applications. *Prog Polym Sci*. 2013;38:1629-52.
- Gazonato EC, Maia AAD, Silva Moris VA, Paiva JMF. Thermomechanical properties of corn starch based film reinforced with coffee ground waste as renewable resource. *Mater Res*. 2019;22(2):1-8. <http://dx.doi.org/10.1590/1980-5373-MR-2018-0416>.
- Wang H, Zhang B, Chen L, Li X. Understanding the structure and digestibility of heat-moisture treated starch. *Int J Biol Macromol*. 2016;88:1-8.
- Manoel AF, Claro PIC, Mattoso LHC, Marconcini JM, Mantovani GL. Thermoplastic waxy starch films processed by extrusion and pressing: Effect of glycerol and water concentration. *Mater Res*. 2017;20:353-7.
- Wang S, Li C, Copeland L, Niu Q, Wang S. Starch retrogradation: A comprehensive review. *Comprehensive Reviews in Food Science and Safety*. 2015;14:568-85.
- Koch K, Gillgren T, Stading M, Andersson R. Mechanical and structural properties of solution-cast high-amylose maize starch films. *Int J Biol Macromol*. 2010;46:13-9.
- Li X, Qiu C, Ji N, Sun C, Xiong L, Sun Q. Mechanical, barrier and morphological properties of starch nanocrystals-reinforced pea starch films. *Carbohydr Polym*. 2015;121:155-62.
- Rocha GO, Farias MG, Carvalho CWP, Ascheri JLR, Galdeano MC. Biodegradable composite films based on cassava starch and soy protein. *Polímeros*. 2014;24:587-95.
- Angellier H, Molina-Boisseau S, Dole P, Dufresne A. Thermoplastic starch: Waxy maize starch nanocrystals nanocomposites. *Biomacromolecules*. 2006;7:531-9.
- Machado BAS, Reis JHO, Da Silva JB, Cruz LS, Nunes IL, Pereira FV, et al. Obtaining nanocellulose from green coconut fibers and incorporation in biodegradable films of starch plasticized with glycerol. *Quim Nova*. 2014;37:1275-82.
- Nascimento P, Marim R, Carvalho G, Mali S. Nanocellulose produced from rice hulls and its effect on the properties of biodegradable starch films. *Mater Res*. 2016;19:167-74.
- Karimi S, Dufresne A, Md. Tahir P, Karimi A, Abdulkhani A. Biodegradable starch-based composites: Effect of micro and nanoreinforcements on composite properties. *J Mater Sci*. 2014;49:4513-21.
- Malucelli LC, Matos M, Jordão C, Lacerda LG, Carvalho Filho MAS, Magalhães WLE. Grinding severity influences the viscosity of cellulose nanofiber (CNF) suspensions and mechanical properties of nanopaper. *Cellulose*. 2018;25:6581-9.
- Fan H, Ji N, Zhao M, Xiong L, Sun Q. Characterization of starch films impregnated with starch nanoparticles prepared by 2,2,6,6-tetramethylpiperidine-1-oxyl (TEMPO)-mediated oxidation. *Food Chem*. 2016;192:865-72.
- Pelissari FM, Andrade-Mahecha MM, Sobral PJA, Menegalli FC. Nanocomposites based on banana starch reinforced with cellulose nanofibers isolated from banana peels. *J Colloid Interface Sci*. 2017;505:154-67.
- Basiak E, Debeaufort F, Lenart A. Effect of oil lamination between plasticized starch layers on film properties. *Food Chem*. 2016;195:56-63.
- Galdeano MC, Wilhelm AE, Mali S, Grossmann MVE. Influence of thickness on properties of plasticized oat starch films. *Braz Arch Biol Technol*. 2013;56:637-44.
- Shankar S, Rhim JW. Preparation of nanocellulose from micro-crystalline cellulose: The effect on the performance and properties of agar-based composite films. *Carbohydr Polym*. 2016;135:18-26.
- Ito VC, Bet CD, Wojeicchowski JP, Demiate IM, Spoto MHF, Schnitzler E, et al. Effects of gamma radiation on the thermoanalytical, structural and pasting properties of black rice (*Oryza sativa* L.) flour. *J Therm Anal Calorim*. 2018;133:529-37.
- Colman TAD, Demiate IM, Schnitzler E. The effect of microwave radiation on some thermal, rheological and structural properties of cassava starch. *J Therm Anal Calorim*. 2014;115:2245-52.
- Cao X, Chen Y, Chang PR, Muir AD, Falk G. Starch-based nanocomposites reinforced with flax cellulose nanocrystals. *Express Polym Lett*. 2008;2:502-10.
- AL-Hassan AA, Norziah MH. Effect of transglutaminase induced crosslinking on the properties of starch/gelatin films. *Food Packag Shelf Life*. 2017;13:15-9.
- Jiang S, Liu C, Wang X, Xiong L, Sun Q. Physicochemical properties of starch nanocomposite films enhanced by self-assembled potato starch nanoparticles. *Lebensm Wiss Technol*. 2016;69:251-7.
- Aila-Suárez S, Palma-Rodríguez HM, Rodríguez-Hernández AI, Hernández-Urbe JP, Bello-Pérez LA, Vargas-Torres A. Characterization of films made with chayote tuber and potato starches blending with cellulose nanoparticles. *Carbohydr Polym*. 2013;98:102-7.
- Versino F, García MA. Cassava (*Manihot esculenta*) starch films reinforced with natural fibrous filler. *Ind Crops Prod*. 2014;58:305-14.
- Ma B, Qin A, Li X, Zhao X, He C. Structure and properties of chitin whisker reinforced chitosan membranes. *Int J Biol Macromol*. 2014;64:341-6.
- Corradini E, Lotti C, Medeiros ES, Carvalho AJF, Curvelo AAS, Mattoso LHC. Estudo comparativo de amidos termoplásticos derivados do milho com diferentes teores de amilose. *Polímeros*. 2005;15:268-73.
- Agustin MB, Ahmmad B, Alonzo SMM, Patriana FM. Bioplastic based on starch and cellulose nanocrystals from rice straw. *J Reinf Plast Compos*. 2014;33:2205-13.
- Dai L, Qiu C, Xiong L, Sun Q. Characterisation of corn starch-based films reinforced with taro starch nanoparticles. *Food Chem*. 2015;174:82-8.
- Salaberria AM, Diaz RH, Labidi J, Fernandes SCM. Role of chitin nanocrystals and nanofibers on physical, mechanical and functional properties in thermoplastic starch films. *Food Hydrocoll*. 2015;46:93-102.
- Salaberria AM, Labidi J, Fernandes SCM. Chitin nanocrystals and nanofibers as nano-sized fillers into thermoplastic starch-based biocomposites processed by melt-mixing. *Chem Eng J*. 2014;256:356-64.
- Li W, Guo R, Lan Y, Zhang Y, Xue W, Zhang Y. Preparation and properties of cellulose nanocrystals reinforced collagen composite films. *J Biomed Mater Res A*. 2014;102:1131-9.
- Nafchi AM, Alias AK. Mechanical, Barrier, Physicochemical, and Heat Seal Properties of Starch Films Filled with Nanoparticles. *Journal of Nano Research*. 2013;25:90-100.
- Mali S, Grossmann MVE, Yamashita F. Starch films: production, properties and potential of utilization. *Semina: Ciênc Agrár*. 2010;31:137-56.
- Chen Y, Yang Q, Xu X, Qi L, Dong Z, Luo Z, et al. Structural changes of waxy and normal maize starches modified by heat moisture treatment and their relationship with starch digestibility. *Carbohydr Polym*. 2017;177:232-40.
- Melo PTS, Aouada FA, Moura MR. Production of Nanocomposite of films of pectin based on cocoa puree with potential use as packaging for food. *Quim Nova*. 2017;40(3):247-51.

39. Zheng H, Ai F, Chang PR, Huang J, Dufresne A. Structure and properties of starch nanocrystal-reinforced soy protein plastics. *Polym Compos.* 2009;30:474-80.
40. Lomelí-Ramírez MG, Kestur SG, Manríquez-González R, Iwakiri S, De Muniz GB, Flores-Sahagun TS. Bio-composites of cassava starch-green coconut fiber: Part II - Structure and properties. *Carbohydr Polym.* 2014;102:576-83.
41. Suwanprateep S, Kumsapaya C, Sayan P. Structure and Thermal Properties of Rice Starch-based Film Blended with Mesocarp Cellulose Fiber. *Materials Today Proceeding.* 2019;17:2039-47.
42. Kubiaki FT, Figueroa AM, de Oliveira CS, Demiate IM, Schnitzler E, Lacerda LG. Effect of acid-alcoholic treatment on the thermal, structural and pasting characteristics of European chestnut (*Castanea sativa*, Mill) starch. *J Therm Anal Calorim.* 2018;131:587-94.
43. García NL, Famá L, Dufresne A, Aranguren M, Goyanes S. A comparison between the physico-chemical properties of tuber and cereal starches. *Food Res Int.* 2009;42:976-82.
44. Montero B, Rico M, Rodríguez-Llamazares S, Barral L, Bouza R. Effect of nanocellulose as a filler on biodegradable thermoplastic starch films from tuber, cereal and legume. *Carbohydr Polym.* 2017;157:1094-104.
45. Wang W, Zhou H, Yang H, Zhao S, Liu Y, Liu R. Effects of salts on the gelatinization and retrogradation properties of maize starch and waxy maize starch. *Food Chem.* 2017;214:319-27.
46. Šárka E, Dvořáček V. Waxy starch as a perspective raw material (a review). *Food Hydrocoll.* 2017;69:402-9.